# Subsurface flow velocities in a hillslope with lateral preferential flow

A. E. Anderson,[1,2] M. Weiler,[3] Y. Alila,[4] and R. O. Hudson[4]

Received 28 April 2008; revised 15 July 2009; accepted 31 July 2009; published 10 November 2009.

[1] Our understanding of hillslope subsurface flow relies on assumptions about how storm characteristics affect the hillslope runoff response. Experiments in hillslopes dominated by preferential flow features often show that runoff is dynamic and is affected by antecedent conditions, rainfall conditions, and position of the slope. We applied tracers to a hillslope under natural and steady state flow boundary conditions to determine the relationship between lateral tracer velocities and various hillslope lengths and storm indicators. Tracer velocities were similar to the fastest velocities measured in other similar experiments. The velocities were dependent on the boundary conditions and slope length, and the subsurface flow velocity was most closely related to the 1-h rainfall intensity. Unlike some studies, there was little correlation between our measured flow velocities and storm volume or antecedent conditions. We attributed this to the hillslope characteristics and the relatively consistent wet antecedent conditions during the experiments. This experiment showed that the connectivity of the hillslope preferential flow network is an important factor governing the average subsurface flow velocity.

**Citation:** Anderson, A. E., M. Weiler, Y. Alila, and R. O. Hudson (2009), Subsurface flow velocities in a hillslope with lateral preferential flow, *Water Resour. Res.*, *45*, W11407, doi:10.1029/2008WR007121.

## 1. Introduction

[2] Subsurface flow in hillslopes dominates the hydrological response and the transport of solutes and nutrients in steep, forested watersheds in humid climates. Decades of hillslope experiments have identified many dominant processes and numerous (sometimes conflicting) conceptual models about the flow features and the mechanisms that control water flow have been developed. Preferential flow has emerged to be an important factor in hillslope hydrology [*Mosley*, 1979]. Lateral preferential flow occurs either in distinctive structures in the soil where water flows only under gravity (macropores or pipes) or in areas with a higher permeability than the surrounding soil matrix [*Weiler et al.*, 2005]. Excavations have found that forested hillslopes in humid climates have relatively short (generally less than 1 m) preferential flow features [*Noguchi et al.*, 1999; *Terajima et al.*, 2000]. Some steep forested hillslopes have been reported to have large preferential flow features, but it is not known how far upslope they extended [*Kitahara*, 1993; *Roberge and Plamondon*, 1987; *Tsukamoto and Ohta*, 1988; *Uchida et al.*, 1999].

[3] Although individual preferential flow features are usually short and discontinuous, fast subsurface velocities and quick runoff responses to precipitation have been observed in many hillslopes [*Hutchinson and Moore*, 2000; *Parlange et al.*, 1989; *Peters et al.*, 1995; *Tani*, 1997]. These fast velocities and subsurface flow responses have led to the idea of a preferential flow network, which describes a series of hydraulically connected preferential features that appear to be physically discontinuous. The exact mechanisms that cause water to move through the preferential network are not well known, but it is often assumed that saturated soil provides the connection between preferential features [*Sidle et al.*, 2001; *Steenhuis et al.*, 1988]. The reasoning behind this assumption is that vertical and lateral redistribution of water within a hillslope raises the soil moisture content, which increases the connections between preferential features and affects the subsurface flow response [*Sidle et al.*, 2000]. Studies have shown that this dynamic subsurface flow response is influenced by antecedent moisture condition, precipitation intensity, precipitation amount, topography, and the physical characteristics of the preferential flow network [*Sidle et al.*, 1995, 2000; *Tromp-van Meerveld and McDonnell*, 2006a; *Tsuboyama et al.*, 1994; *Uchida et al.*, 2005].

[4] Physically based, numerical models are often used for predicting the effects of land use changes on watershed hydrology and for testing hypotheses of watershed behavior. Successful modeling requires a good understanding of the processes and mechanisms that affect the dynamics in the system [*Sidle*, 2006; *Weiler and McDonnell*, 2004]. Preferential flow models have been developed for a single pipe [*Tsutsumi et al.*, 2005], for hillslopes [*Faeh et al.*, 1997; *Weiler and McDonnell*, 2007], and for watersheds [*Beckers and Alila*, 2004]. The subsurface water velocity is usually the primary parameter used (directly or indirectly) to simulate subsurface flow and solute transport. Most hillslope- and watershed-scale models are developed using a small number

[1]Sustainable Resource Development, Calgary, Alberta, Canada.
[2]Department of Civil Engineering, University of Calgary, Calgary, Alberta, Canada.
[3]Institute of Hydrology, Albert-Ludwigs University of Freiburg, Freiburg, Germany.
[4]Department of Forest Resources Management, University of British Columbia, Vancouver, British Columbia, Canada.


0043-1397/09/2008WR007121

of velocity measurements at a small scale [*Beckers and Alila*, 2004] or relationships developed for single preferential features [*Weiler and McDonnell*, 2007].

[5] Artificial and natural tracers have been used to quantify hillslope response under natural and steady state conditions. Conservative anion tracers such as chloride and bromide are often used successfully [*Feyen et al.*, 1999; *Kung et al.*, 2005, 2006; *Nyberg et al.*, 1999; *Tsuboyama et al.*, 1994]. Depending on the experimental design, tracers are used to determine the vertical, lateral, or combined vertical and lateral velocity of subsurface water. Tracers are applied during steady state (generally sprinkling or pumping) or natural conditions. However, steady state experiments are preferred because they are simpler to analyze and interpret [*Tsuboyama et al.*, 1994].

[6] In this paper, results from a hillslope-scale experiment under different boundary conditions are presented. Artificial tracer (NaCl) was applied under natural and steady state lateral flow conditions to determine the effect of slope length and flow rate on the velocity of lateral subsurface flow. The experimental hillslope was gauged at a road cutbank from February to June 2005 to examine the behavior of water and applied tracers in outflow from preferential flow features and the soil matrix under natural conditions. These data were used to determine velocities that describe the transport of solute from the soil surface to the road cut during different storms. Following the experiments conducted under natural conditions, steady state experiments were conducted to determine the lateral tracer velocities for different flow rates and different hillslope lengths (12 m and 30 m). Specifically, this paper attempts to determine patterns between subsurface flow velocity and various parameters including precipitation characteristics, antecedent soil moisture and pore water pressure. We then discuss how these relationships conform to conceptual models of preferential flow networks in hillslopes.

## 2. Methods

### 2.1. Study Site

[7] The experiments were conducted in the 30-km$^2$ Russell Creek research watershed located in northeastern Vancouver Island, British Columbia, Canada. The watershed ranges in elevation from 275 to 1715 m above sea level (asl), which places the majority of the watershed into the rain-on-snow zone (300–800 m) and the snow zone (above 800 m). This area has high annual precipitation. Average precipitation at two gauges in the watershed was 2258 mm/yr (average 1995–2000) at 830 m asl and 1906 mm/yr (average 1991–2000) at 300 m asl, with the majority of the precipitation falling in the winter months (80% of total precipitation between September and April). Russell Creek is a typical coastal British Columbia rain-on-snow-dominated watershed, but its drainage area is large in comparison to catchments that are typically used for intensive process-based research. The average slope of Russell Creek is 47%. A 2.3-km$^2$ subbasin of the Russell Creek watershed (hereby named Axel Creek) with gentler topography (average slope 37%) was selected in order to study hillslope and watershed processes at a scale more suitable to intensive research (Figure 1). Note that there is an order of magnitude difference in watershed areas. Prior to embarking on the study described herein, a 20-ha part of Axel Creek was intensively instrumented with piezometer transects and stream gauges to study the effects of forest roads on hillslope hydrology.

[8] In the Russell Creek watershed, forest roads were mainly constructed along hillslopes, which resulted in many road cutbanks intersecting the entire soil profile and part of the till or bedrock. After months of observing stormflow exiting from hillslopes at road cutbanks in Axel Creek and elsewhere, and following preliminary experiments conducted in the summer of 2004, a typical hillslope section was selected and gauged at a road cutbank (Figure 1). The outflow face at the cutbank was 9 m wide at an elevation of 400 m asl and produced concentrated flow at the road cutbank during storms. This hillslope was chosen because it was found to typify the soil, vegetation, and flow characteristics of hillslopes in Axel Creek (and, by extension, in Russell Creek watershed), and because the site was within 300 m of meteorological instrumentation and gauged streams, and was adjacent to one of the piezometer transects. We expected relatively easy winter access because the road was in good condition and experienced only an intermittent snowpack.

[9] The gauging site collected water from a moderately steep (30% gradient) hillslope approximately 100 m long (Figure 1). The topography of this hillslope was undulating with wet hollows and drier convex ridges. The moisture regime was indicated by changes in vegetation and soil characteristics. Soil characteristics were observed at the road cutbanks, during piezometer installation, and during excavations. In general, the soils were 0.5–2 m deep. The tracer experiments focused on the lower 30 m of the hillslope. This 30-m section covered two small-scale topographical units and soil characteristics commonly found at Russell Creek. The lower bounding layer for the entire experimental site consisted of till that was assumed impermeable for the purpose of this study. A 300-year-old, 200-cm diameter, 47-m-tall stand of Western Hemlock (*Tsuga heterophylla*) and Amabilis Fir (*Abies amabilis*) covered the whole hillslope (stand information from inventory and observations).

[10] The center of the lower 10–15 m of the hillslope (above S2 in Figure 1) was typical of topographical hollows with organic and clay-rich soils (Bg and Ah) less than 1 m deep. The remainder of the hillslope (above S1 and S3, and above 15 m, Figure 1) was typical of convex hillslopes, with soils of 1- to 1.5-m depth that had a 5- to 35-cm-thick Ae layer, and a Bf layer approximately 1 m deep.

### 2.2. Basic Instrumentation

[11] There are five mainstream gauges in Russell Creek that are continuously monitored for flow, using salt dilution gauging at channel control gauging reaches. At Axel Creek, gauging sites were located at the main stem channel above Russell Creek, at its tributaries and at ditches flowing into the tributaries. All flow measurement sites were gauged using sharp-crested V notch plywood weir boxes and water levels in the weir boxes were monitored using standalone Odyssey capacitive water depth probes.

[12] A total of 35 piezometers were installed in Axel Creek watershed, of which eight were located within the experimental hillslope. It is noted that while a piezometer measures pressure head at the completion interval, under lateral subsurface flow conditions the pressure head is equivalent to the water table height. Piezometers were constructed in situ from

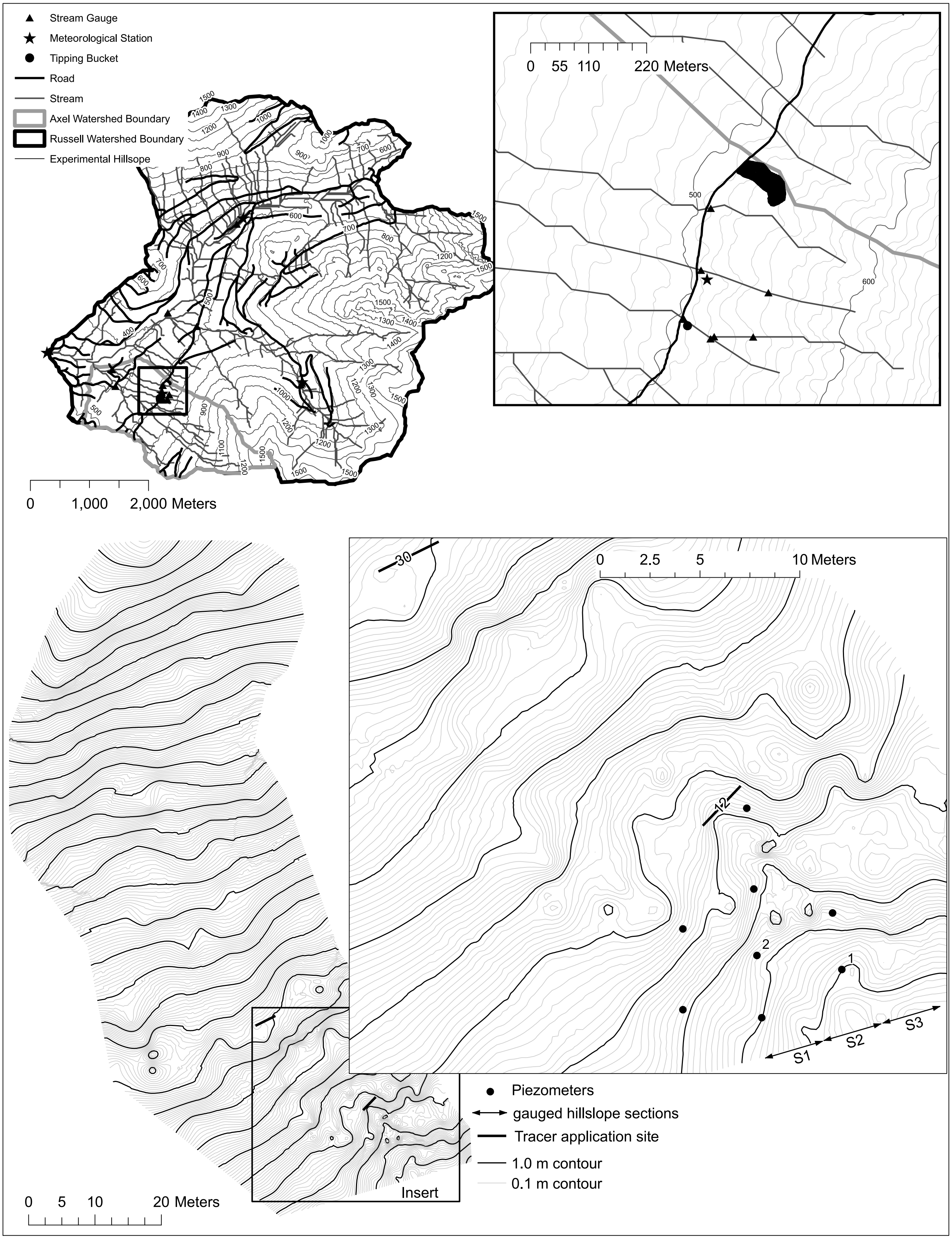


**Figure 1.** Contour map of the experimental hillslope developed from a total station survey showing the tracer injection sites, piezometer locations, and the gauged sections.

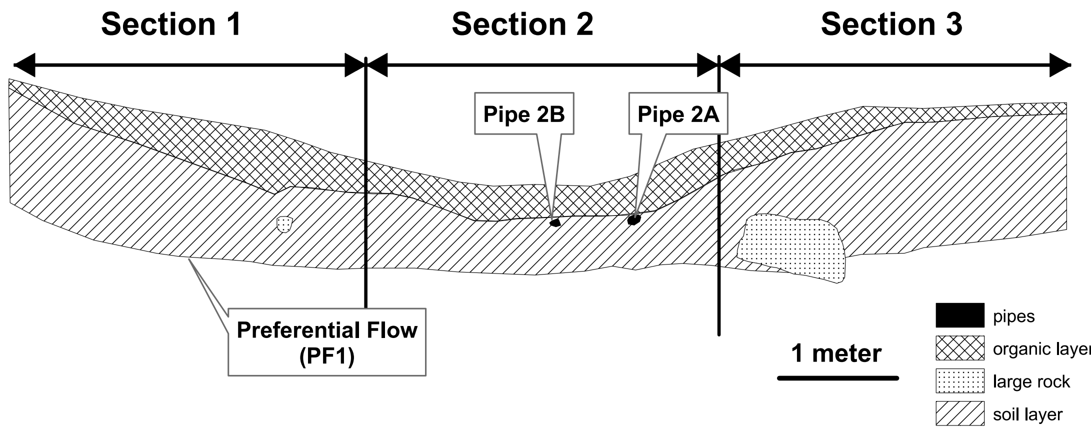


**Figure 2.** Diagram of the hillslope outflow face showing the three gauged sections and the three individually gauged features: (1) pipe 2A, (2) pipe 2B in section 2, and (3) preferential flow at the interface of the till and soil in section 1.

2.5-cm-diameter PVC pipe with a 30-cm completion interval at the bottom of the pipe. The completion interval was isolated with bentonite clay, the hole was partially backfilled with gravel and capped with concrete. In two of the piezometers (P1 and P2) within the experimental hillslope Unidata Hydrostatic Water Depth and Temperature Probes (model 6542) connected to a Unidata Starlog data logger monitored and recorded water levels every 5 min. For purposes of this study, groundwater fluctuations during storms were inferred from Piezometers P1 and P2, which were 1000 and 950 mm deep, respectively (Figure 1). The six other piezometers installed in the hillslope ranged in depth from 860 to 1400 mm. Slug tests were performed on all eight piezometers to determine hydraulic conductivity (K) according to the Hvorslev method. Six of the piezometers had K values between 0.1 and $1.4 \times 10^{-6}$ m/s. Similar to other sites [*Kim et al.*, 2004], two piezometers drained too quickly to complete the slug tests.

### 2.3. Hillslope Experiment Setup

[13] To measure outflows from the hillslope, the 9-m road-cut section of the outflow face was divided into three subsections (S1, S2, and S3), each 3 m wide. The outflows from each section were measured and recorded as described below. Three preferential flow features were also gauged (pipe 2A, pipe 2B, and PF1 in Figure 2).

[14] Concrete troughs at the road cut collected the water draining from the three sections (Figure 2) and diverted the water into 7.5-cm-diameter ABS pipes. Concrete was also used to seal ABS pipes into the preferential flow features. The ABS pipes carried the water into tipping buckets constructed from sheet aluminum and mounted on a level platform. Magnetic reed switches connected to a Campbell Scientific CR10 data logger monitored the tipping buckets and recorded the number of tips per minute. The tipping buckets were initially calibrated with a 1 liter graduated cylinder. After the experiments were complete water was pumped at specific flow rates into each tipping bucket to determine the effect of the flow rate on tipping capacity. The tipping bucket capacities ranged from 0.80 to 1.06 L/tip and the flow rate did not significantly affect the tipping capacity. The instruments were shielded from rain, snow and wind by walls and a roof.

[15] Preferential flow was observed at the interface of Bf layer and the till in S1 (PF1 in Figure 2). We also suspected that preferential flow might occur around some large roots that were found in the Bf layer of S1 (upper left corner of Figure 2). However, it was not possible to isolate all the preferential flows from S1 other than those from PF1, which we measured. We therefore assumed a proportion of the water measured from S1 to be supplied by preferential flow.

[16] S2 was located below a topographical hollow. In this section of the outflow face, the clay content of the soil was higher than other parts of the hillslope. The piezometers installed in this part of the hillslope also had lowest measurements of hydraulic conductivity (1.3 and $1.7 \times 10^{-7}$ m/s, which is 1 order of magnitude lower than the highest measured at this site). The soils had a 30-cm Ah layer and a 30- to 50-cm Bg layer. In this section there were two large soil pipes (pipe 2A and pipe 2B, Figure 2). Pipe 2A was 10–12 cm in diameter and was connected to highly conductive features, creating a preferential flow network that extended 10 m up slope (determined by a subsequent dye staining and excavation experiment [*Anderson et al.*, 2009]). Pipe 2B was 5–8 cm in diameter and was less well connected than pipe 2A. Both pipes were near the interface of the organic Ah layer and the Bg layer. Gravel of 2- to 5-mm diameter was found deposited on the bottom of both soil pipes and old bark from decayed tree roots lined the top and sides of pipe 2B.

[17] Using the experimental setup described above, two types of tracer experiments were conducted: forced and natural. Forced experiments were conducted under steady state (i.e., constant) water flow conditions. Although the tracer movement did not achieve steady state conditions, conservation of tracer mass and constant flow rate of water through the soil could be assumed, simplifying the analysis and interpretation of the experimental data. However, because the flow conditions were "forced" (i.e., induced by ponded water in trenches), they represent subsurface flow conditions that would not likely occur naturally during storms. Therefore, the natural condition experiments were conducted to infer flow rates through soil matrix and through preferential flow paths under real conditions during specific storms, using the results of the forced experiments to interpret the data. The natural condition experiments were conducted first, followed by the forced experiments.

**Table 1.** Natural Event Total Discharge and Percentages of the Total Discharge for the Six Gauges[a]

| | Start Date | Total Precipitation (mm) | Total Flow ($m^3$) | 7-Day Antecedent Rainfall (mm) | Section 1 (%) | Preferential 1 (%) | Section 2 (%) | Pipe 2A (%) | Pipe 2B[b] (%) | Section 3 (%) |
|---|---|---|---|---|---|---|---|---|---|---|
| Event 1 | 7 Mar | 14 | 16.3 | 35 | 5.0 | 9.5 | 1.2 | 66.0 | 15.2 | 3.1 |
| Event 2 | 10 Mar | 10 | 0.5 | 65 | 8.9 | 7.5 | 20.4 | 45.7 | 8.6 | 8.8 |
| Event 3 | 16 Mar | 27 | 5.8 | 55 | 7.0 | 9.8 | 5.1 | 66.8 | 4.2 | 7.0 |
| Event 4 | 25 Mar | 41 | 29.1 | 39 | 9.7 | 16.0 | 1.7 | 57.9 | 8.8 | 6.0 |
| Event 5 | 30 Mar | 87 | 98.0 | 60 | 11.3 | 10.3 | 1.5 | 61.0 | 11.0 | 4.9 |
| Event 6 | 5 Apr | 104 | 97.6 | 108 | 18.7 | 7.5 | 2.2 | 58.0 | 9.8 | 3.8 |
| Event 7 | 10 Apr | 19 | 1.8 | 154 | 45.5 | 13.3 | 2.9 | 29.0 | 3.9 | 5.4 |
| Event 8 | 15 Apr | 45 | 49.6 | 98 | 11.0 | 11.8 | 1.9 | 61.7 | 9.1 | 4.5 |
| Event 9 | 10 May | 27 | 2.0 | 4 | 0.2 | 0.1 | 5.6 | 82.8 | 11.3 | 0.1 |
| Event 10 | 14 May | 15 | 0.8 | 36 | 0.0 | 0.0 | 12.1 | 72.8 | 14.8 | 0.2 |
| Event 11 | 18 May | 58 | 33.0 | 49 | 8.5 | 18.2 | 1.3 | 66.2 | | 5.8 |
| Event 12 | 21 May | 92 | 81.3 | 104 | 29.2 | 8.2 | 2.5 | 56.2 | | 3.9 |
| Event 13 | 17 Jun | 16 | 10.8 | 36 | 8.8 | 22.2 | 2.1 | 64.0 | | 2.9 |
| Average outflow | | | | | 12.6 | 10.4 | 4.7 | 60.7 | 9.7 | 4.3 |

[a]Total flow was calculated as the amount of flow above the flow before the start of the response to rainfall.
[b]The Pipe 2B tipping bucket was damaged during the 18 May storm, and three storms were missed. Note that the average storm outflow percentages do not sum to 100, because they are the average of the percent contribution per storm. Storm 3 includes snowmelt.

### 2.4. Application and Outflow Detection of Tracer Under Natural Conditions

[18] Dry NaCl tracer was applied to the soil surface along line sources on two occasions. On 7 March, 10 kg of tracer were applied at 12 m above the road (the 12-m experiment), and on 31 March, 20 kg were applied at 30 m above the road (the 30-m experiment). Locations of the line sources are shown in Figure 1. The relatively large quantity of tracer was used because we expected the tracer to be highly diluted and because each application of the tracer was required to last through several storms. The 12-m application lasted through five storms with a total of 179 mm of precipitation (Table 1). At the end of the 12-m experiment in late March, the measured breakthrough signal was weak, but the quantity of tracer recovered indicated that there was still considerable residual tracer diffused into the soil matrix. Therefore for the 30-m experiment we doubled the quantity of tracer to ensure a strong signal to overwhelm the diluted residual tracer in the lower 12 m of the slope. The 30-m application lasted through eight storms with a total of 376 mm of precipitation (Table 1). It is recognized that $Na^+$ applied in large quantities to soil can act as a dispersion agent and while the quantities of tracer used in this experiment may seem excessive, it is clear that only a portion of the salt was mobilized by each storm event. Large amounts of tracer have been used successfully in other soil tracer experiments [*Kienzler and Naef*, 2008; *Ronkanen and Klove*, 2007].

[19] We used electrical conductivity (EC) probes to detect the tracer in outflows. We were able to use EC because of the strong linear relation between ion concentration and the relatively low and constant ion concentration in background hillslope water in Russell Creek. A large number of EC probes were required for the experiment, and owing to budgetary constraints, we construct EC and temperature probes using a design similar to the Campbell Scientific CS547A-L. These probes were connected to Campbell Scientific CR10 data loggers to measure the electrical conductivity and temperature of the water draining from the outflow face into the tipping buckets.

[20] We calibrated the probes first to EC (using a laboratory EC probe) and then to NaCl concentration (mg/L) using a set of ten standard NaCl solutions made with distilled water. The relationship between concentration and EC is affected by both temperature and by the ionic strength and chemical signature of the native water [*Hudson and Fraser*, 2005]. To compensate for chemical effects at the site, an alternate set of solutions was made with water collected from the experimental site during different runoff conditions. These solutions were then used to establish site-specific temperature compensation relations in the range of 1–5°C. This is the range in which those relations are typically nonlinear [*Hudson and Fraser*, 2005]. Coefficients of determination for these relationships varied from 0.96 to 0.99 depending on the probe and the range of EC. The EC and chloride calibrations were periodically checked with a laboratory conductivity probe and with the standard solutions. The background measurements may have included residual tracer left over or stored from earlier applications. Background EC levels were very low and relatively constant during storms (less than 20 $\mu$S/cm) and were subtracted from the measurements to yield only the concentration due to the applied tracer.

### 2.5. Forced Tracer Experiments

[21] During dry conditions in July 2005, two trenches 4 m long, 30 cm wide, and ranging in depth from 30 to 50 cm were excavated to the till layer at the same locations where the tracer was applied to the soil surface for natural condition experiments (12 and 30 m above the road, Figure 1). Two experiments were conducted at each trench. These experiments were named 12-m high rate (12 mHR), 12-m low rate (12 mLR), 30-m high rate (30 mHR), and 30-m low rate (30 mLR). The 12-m experiments were conducted first. The goal was to have the high-flow-rate experiments mimic the highest hillslope flow rates observed during the natural storms (30.8 L/min for the large Pipe 2A, Figure 2). However, a maximum rate of only 29.1 L/min and 23.5 L/min was achieved for the 12 mHR and 30 mHR, respectively, before the trenches were overtopped. The low pumping rates, chosen to be approximately 50% of the maximum rates, were 15.2 L/min for the 12 mLR and 14.0 L/min for the 30 mLR.

[22] Water from a nearby stream was diverted into the trench using a 2.5-cm-diameter, 300-m-long polyethylene

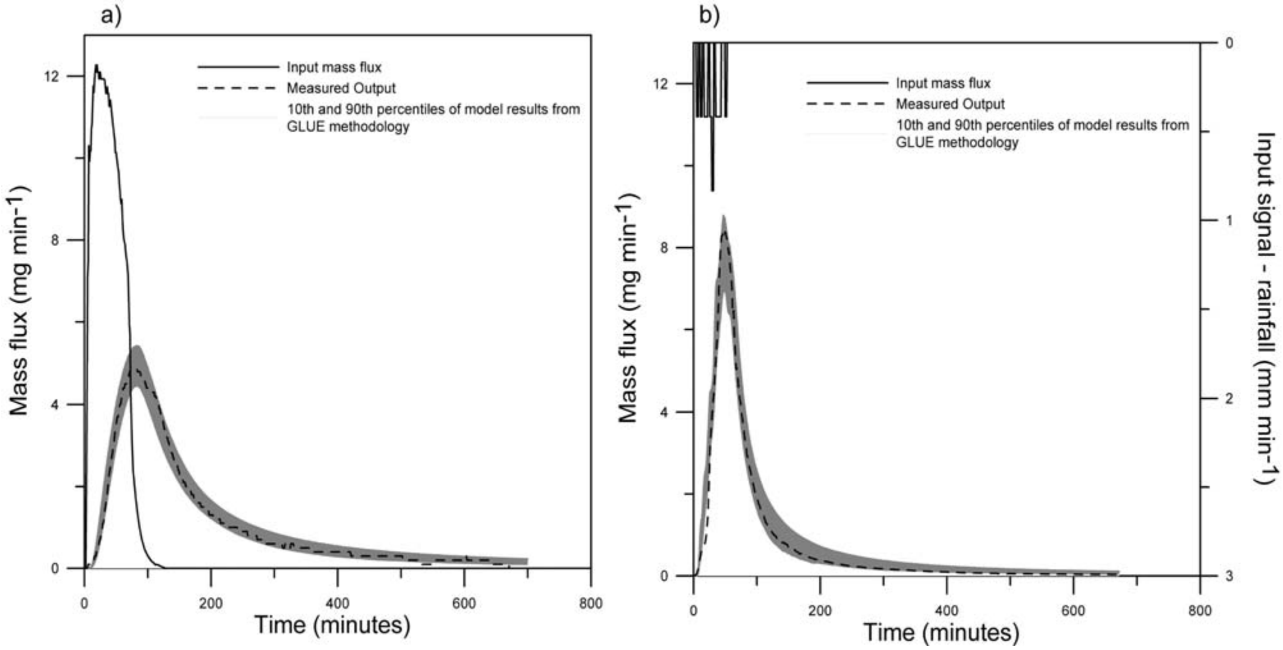


**Figure 3.** (a) Example of 12-m low-rate forced tracer experiment for Pipe 2B. Tracer input mass flux is scaled so the total input mass equals output mass. (b) Example of 12-m natural experiment, storm 1. Tracer mass input signal is scaled to the rainfall. GLUE, general likelihood uncertainty estimation.

pipe. Steady state flow conditions were assumed when the outflow rate equaled the input flow rate and a constant outflow rate was measured with each of the tipping buckets at the base of the hillslope. Once the outflow of the hillslope had reached steady state, a pulse of NaCl solution (3 g/L) was mixed into the water flowing into the trench at a constant rate of 0.1 or 0.2 L/min (for the low- and high-flow rates, respectively) over a period of 3–6 h (for the 12-m and 30-m experiments, respectively). The constant injection rate was maintained using a Mariotte bottle constructed from a 200-L container. The NaCl concentrations in the input trenches and the outflow were measured with the same conductivity probe setup used in the natural tracer experiments. The time to steady state ranged from approximately 15 min for the 12 HR to over 1 h for the 30 mLR to achieve steady state; however the hillslope were maintained at steady state for a minimum of 2 h before the tracer was added. All experiments lasted 22 to 24 h.

### 2.6. Analysis of Data From Forced Experiments

[23] For the steady state flow experiments, the tracer added to the input trench had to mix with the water in the trench, which changed the input, so the tracer input was no longer a well-defined pulse. A transfer function was used to transform the input signal to the output signal, as follows:

$$d_{out}(t) = \int_0^\infty g(t')d_{in}(t-t')dt', \tag{1}$$

where *g(t)* is the response function or the distribution of transit times ($t'$) and $t$ is real time [*Roth and Jury*, 1993]. A Monte Carlo approach was used to determine velocity and dispersion coefficients for an advection-dispersion equation:

$$p(t') = \frac{e^{-1\left(1-t'/t'_t\right)^2/\left(4/P_e t'/t'_0\right)}}{\sqrt{4\pi/P_e\left(t'/t'_t\right)^3}}, \tag{2}$$

where $t'_t$ is average travel time through the system and $Pe$ is the Peclet Number [*Maloszewski*, 1994]. The optimal set of coefficients (velocity and dispersion) was determined with the Nash-Sutcliffe coefficient of efficiency [*Nash and Sutcliffe*, 1970].

[24] General likelihood uncertainty estimation (GLUE) methodology was used to determine the sensitivity of the coefficients and establish confidence bounds [*Beven and Freer*, 2001]. Following the approach by *Zhang et al.* [2006], Monte Carlo simulations were used to produce 500 sets of coefficients that had Nash-Sutcliffe efficiencies of at least 0.05 less than the optimal solution. The 500 models were weighted by the efficiency results and used to determine a cumulative distribution for each time interval. Figure 3 presents an example of the input and output signal for the 12-m tracer experiment for the output signal for Pipe 2B.

### 2.7. Analysis of Natural Storm Tracer Data

[25] During the natural storms the input of tracer was not known. The NaCl tracer was applied to the soil surface and it was assumed that during each storm, rainfall mobilized a portion of the tracer that was proportional to the rainfall intensity. The rainfall was used as the input signal and the output was the mass flux for the entire hillslope measured at the outflow face (mg/min). The same GLUE methodology was applied to fit coefficients to equations (1) and (2). Figure 3b presents an example of the input-output signal

and the results from the multiple models fitted with the GLUE methodology.

[26] The time series was divided into 13 individual events (Table 1), which ranged in size from 10 to 123 mm of rain. The start of an event was taken as the start of the rainfall that was found to induce an outflow response from the hillslope, and the end of an event was considered to be the start of the next rainfall that produced an outflow response.

[27] To determine relationships between subsurface flow velocities and rainfall and moisture characteristics, the calculated velocities were plotted against several flow and storm parameters, including the average flow rate, total rainfall, 1-h precipitation intensity, antecedent rainfall indices and pressure head measurements of piezometers P1 and P2. Rainfall was measured with two tipping bucket gauges, installed in a clearing approximately 200 m from the gauged hillslope.

[28] Because of the relatively poor correlation between subsurface flow velocity and storm parameters, a multiple regression analysis was undertaken to determine if there was an interaction between parameters that would better explain the velocities (i.e., result in a relation with an improved $R^2$). Multiple regression analysis was done with Minitab version 10X statistical software [*Minitab Inc.*, 1995].

## 3. Results

### 3.1. Hillslope Subsurface Flow Response

[29] Thirteen events between March and June 2005 were identified, ranging in rainfall amount from 10 to 104 mm and outflow volume from 0.5 to 100 $m^3$ (calculated as the sum of the outflow greater than the outflow rate before the start of the event) from the 9-m hillslope outflow face at the road cut (Table 1). All the events were rainstorms (determined by comparing total precipitation gauge and tipping bucket measurements), with the exception of storm 3, which was a rain-on-snow event.

[30] An average of 63.3% of the total outflow was collected from pipe 2A. Pipe 2B and PF1 produced on average 10.3% and 10.1% of the outflow, respectively. S2 and S3 produced 4.8% to 4.2% and S1, 9.9% of the average outflow. However, the outflow rate of S1 increased dramatically during some large storms (Figure 4), which caused an increase in the percentage of outflow in those storms.

### 3.2. Tracer Recovery

#### 3.2.1. Forced Conditions

[31] The 12-m forced experiments (12 mHR and 12 mLR) produced a concentrated response in section S2. Both experiments produced very similar responses for pipe 2A. However, more of the tracer (98.9% versus 97.5%, Table 2) and water (97.4% versus 96.5%, Table 3) was recovered from pipe 2A during the 12 mLR tests as compared to the 12 mHR. To offset the reduction in tracer and water from pipe 2A during 12 mHR, pipe 2B had twice the amount of tracer recovered (1.1% and 2.4%, Table 2), and more water (3.1% and 2.1%, Table 3). S3 had less than 1% of the tracer and water recovered for all experiments (Tables 2 and 3).

[32] Even though most tracer was recovered in the large pipe 2A during the 30-m tracer experiments, more tracer and water were recovered from other sections. Pipe 2A transmitted 82.9% and 88.1% of tracer (Table 2) and 84.7% and 85.9% of the water (Table 3) during 30 mHR and 30 mLR, respectively. Pipe 2B transmitted a higher percentage of the tracer (7.4% and 9.1%, Table 2) during the 30-m experiments than during the 12-m experiments. For the 30-m trench, increasing the flow rate caused less tracer to be recovered from pipe 2A and pipe 2B (97.2% versus 90.3%, Table 2) and more tracer to be recovered from S1 and PF1 (9.3% versus 2.8%, Table 2). Similarly the water recovered from S2 decreased and the water recovered from S1 increased when the pumping rate was increased (Table 3).

#### 3.2.2. Natural Conditions

[33] From the 12-m and 30-m tracer experiments, 19.8% and 24.2% of the applied tracer was recovered at the base of the hillslope (Table 4). Of the recovered tracer, almost the entire (99.1%) NaCl tracer from the 12-m experiment was recovered in Pipe 2A and Pipe 2B (Table 4). For the 30-m experiment, only 77% of the tracer was recovered from pipe 2A, compared to 94.7% for the 12-m experiment (Table 4). The quick breakthrough of tracer, observed almost immediately following the application of NaCl in the 12-m experiment, was not observed in the 30-m experiment (Figure 4).

### 3.3. Tracer Velocities

#### 3.3.1. Forced Conditions

[34] The water in the trench was maintained at a constant level during the experiments. Tracer velocities were inferred from each section and preferential feature where tracer was recovered at the road cut. These tracer velocities do not reflect the velocity through the feature, but integrate the mean velocity of the water and tracer along its flow path through the hillslope to the outflow face at the road. In general, the velocities for the entire hillslope are dominated by flow through pipe 2A because it carries the majority of the tracer during all experiments (82.9–98.9%, Table 2). The 30-m experiments produced a mean hillslope velocity that was over an order of magnitude lower than the velocities produced by the 12-m experiment (Figure 5).

[35] The 12-m tests (both low- and high-flow rates) indicated tracer velocities in pipe 2A that were 1–2 orders of magnitude faster than the velocities measured in all other sections (Figure 5). Similar to the 12-m tests, the 30-m tests indicated that pipe 2A had the highest velocities. For the 30 mHR test the pumping rate was 23.5 L/min, and the test produced tracer velocities that were on the order of $10^{-3}$ and $10^{-4}$ m/s for all gauged features (Figure 5). For the 30 mLR test, the pumping rate was reduced to 14.0 L/min, or 59% of the 30 mHR rate. However, the resulting velocities were reduced by only 15–25% (Figure 5) with the exception of Pipe 2B, which experienced no significant change in velocity when the flow rate was varied.

#### 3.3.2. Natural Conditions

[36] The natural condition tracer velocities are given (Table 5) along with several related parameters. Figure 6 shows the velocity plotted against the average outflow volumes for each storm and the forced experiments. Figure 7 shows the velocity plotted against the 1-h rainfall intensity and the total rainfall amount. Figure 8 shows the velocity plotted against the maximum pressure head in piezometers 1 and 2 for each storm. The parameters most closely related to the hillslope subsurface flow velocity are the maximum height of the water table in piezometer 2 and the 1-h maximum precipitation intensity (Figures 7 and 8). Although not shown, the Peclet number coefficients sug-

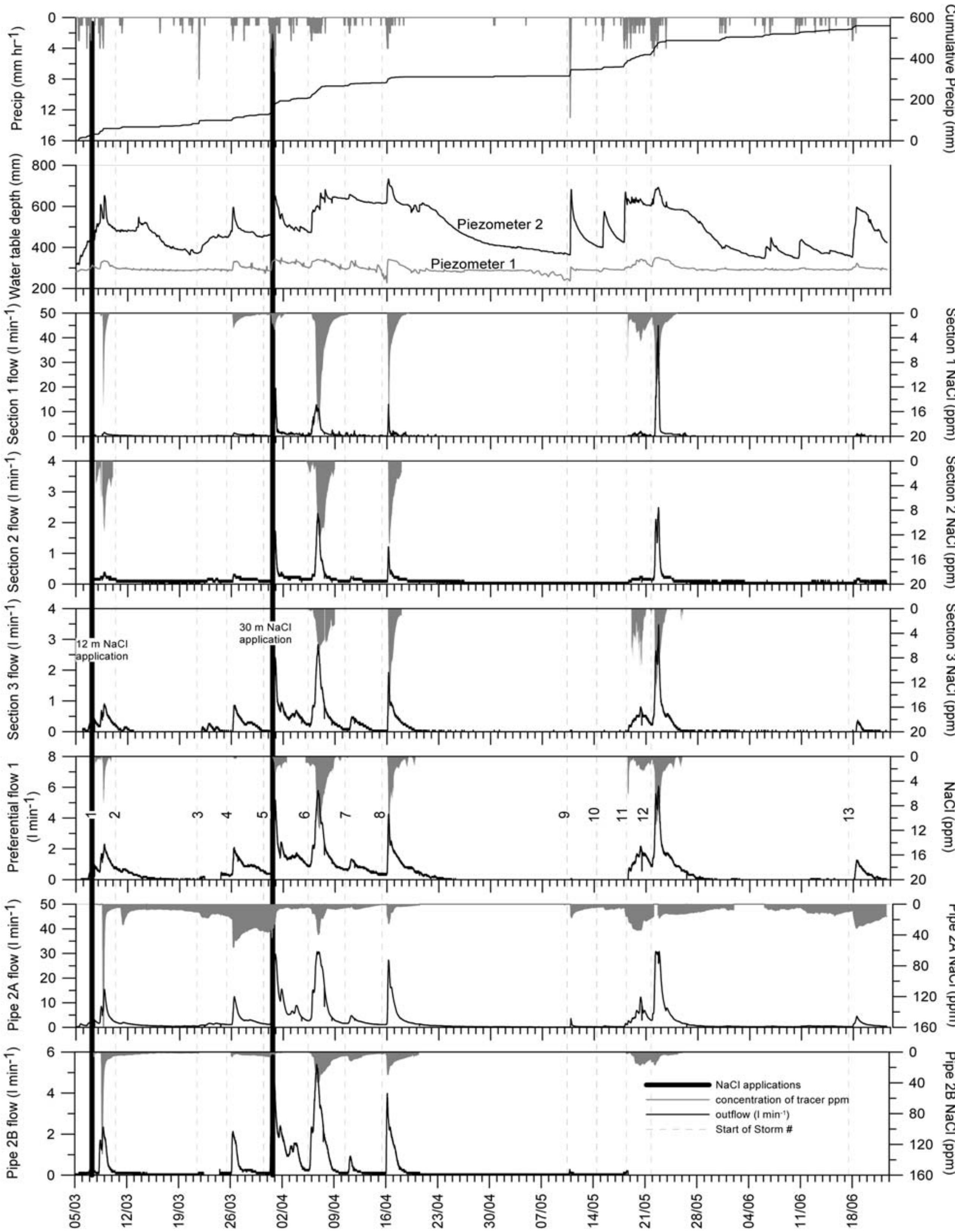


**Figure 4.** Natural event outflow and concentration of tracer for the six gauged sections and two piezometer responses.

**Table 2.** Forced Experiment Measured Tracer Recoveries in Grams and Expressed as Percents of the Total Mass Recovered

| Experiment | Measured Output[a] (NaCl g) | Section 1 (NaCl g) | Preferential 1 (NaCl g) | Section 2 (NaCl g) | Pipe 2A (NaCl g) | Pipe 2B (NaCl g) |
|---|---|---|---|---|---|---|
| 12-m high rate | 461.3 | | | 0.7 (0.2%) | 449.7 (97.5%) | 10.9 (2.4%) |
| 12-m low rate | 909.4 | | | 0.7 (0.1%) | 899.1 (98.9%) | 9.6 (1.1%) |
| 30-m high rate | 430.7 | 13.1 (3.0%) | 27.2 (6.3%) | 1.6 (0.4%) | 356.9 (82.9%) | 31.9 (7.4%) |
| 30-m low rate | 648.2 | 5.7 (0.9%) | 12.2 (1.9%) | 0.8 (0.1%) | 570.8 (88.0%) | 58.7 (9.1%) |

[a]Recovered output was 100% for all tests (within the measurement error).

gested a reduction in dispersion as the average velocity increased.

[37] Subsurface flow velocities (V) were found to be highly correlated with the 1-h rainfall intensity (R1; r = 0.714) but poorly correlated with the 7-day antecedent precipitation index (API; r = 0.061), which was the best of the indices of antecedent moisture condition that we tested. However, other studies [e.g., *Sidle et al.*, 2000] found that subsurface flow volume is related to antecedent moisture condition, so a multiple regression was attempted to determine if a potential interaction between R1 and API might exist. While the results of the analysis suggested that API was not significant in the equation (Table 5), a plot of the measured velocity against the velocity calculated from the regression equation ($V_{calc}$) suggested that there may be two different groupings of storms with responses to R1 and API that are parallel, but offset by a constant value (Figure 9). Using a classification variable (D) to distinguish the two groups, the resulting regression equation becomes highly linear with an $R^2$ of 0.966 (Table 6 and Figure 9). In this analysis, D is the most significant parameter and API is the least (according to their *t* ratios). API is only marginally significant depending on what level of type-1 error is considered acceptable.

## 4. Discussion

### 4.1. Comparison to Other Hillslope Tracer Tests

[38] Tracer studies have been used to quantify the subsurface flow velocity of hillslopes with preferential flow in many areas around the world. To place our results in a global context, we compared our average measured subsurface flow velocities to those measured at forest and grassland sites around the world (Table 7). Our results are among the highest velocities reported in Table 7 and are comparable to those measured at Maimai in New Zealand [*Mosley*, 1979] and at Carnation Creek, west Vancouver Island [*Hetherington*, 1995]. Mosley and Hetherington measured velocities on the order of 100 m/h, which are similar to the velocities measured in the 12-m forced tracer experiments. *Hetherington* [1995] simultaneously measured velocities at another site that was similar in terms of soil characteristics and topography to the section above the 12-m tracer injection trench of our study site, and measured velocities on the same order of magnitude (10 m/h) as the 30-m forced experiments presented here. This suggests that the humid climate (greater than 2000 mm/yr of precipitation), shallow soils (often less than 1 m deep) and lush vegetation of these regions may cause highly developed preferential flow networks in areas with concentrated subsurface flow, resulting in very high local subsurface velocities.

[39] These results also highlight the importance of the length of hillslope used for the experiments. The 12-m forced experiment produced velocities that were higher than any calculated from the tracer application under natural conditions.

### 4.2. Spatial Scale and Boundary Conditions

[40] Higher velocities and different discharge-velocity relationships were measured for the 12-m forced experiments than for the natural storms or the 30-m experiments, which included the 12-m section. With the shorter distance (12 m) the tracer was injected directly into a highly connected preferential flow network that hydraulically connected the input trench with the outflow site [*Anderson et al.*, 2009]. Forced experiments over the longer distance (30 m) and during the natural condition experiments (where dry NaCl was applied to the surface) measured velocities through a less hydraulically connected system and produced much slower responses [*Anderson et al.*, 2009]. This highlights the role that the connections between the preferential flow features play in governing the subsurface flow velocity. This connectivity may have been a factor in other experiments as well. *Mosley* [1979] and *Hetherington* [1995] both measured velocities over a relatively short distance (3 and 4 m), which would increase the likelihood that their experiments measured a highly connected preferential network, as found at the Russell Creek site during excavations [*Anderson et al.*, 2009]. A larger spatial scale experiment or an experiment that included the vertical percolation of a tracer might produce very different results. Studies of vertical macropores have produced similar results, where the length and connection of a single vertical preferential feature had a large influence on the observed vertical flow rate.

[41] In addition to the two slope lengths and different boundary conditions, these experiments were conducted

**Table 3.** Forced Experiment Pumping Rates and Outflows Expressed in L/min and as Percentages of the Total Output

| Experiment | Total Flow Rate (L/min) | Section 1 (L/min) | Preferential 1 (L/min) | Section 2 (L/min) | Pipe 2A (L/min) | Pipe 2B (L/min) |
|---|---|---|---|---|---|---|
| 12-m high rate | 29.10 | | | 0.12 (0.4%) | 28.09 (96.5%) | 0.89 (3.1%) |
| 12-m low rate | 15.16 | | | 0.08 (0.5%) | 14.77 (97.4%) | 0.31 (2.1%) |
| 30-m high rate | 23.48 | 0.63 (2.7%) | 1.25 (5.3%) | 0.15 (0.6%) | 19.90 (84.7%) | 1.55 (6.6%) |
| 30-m low rate | 13.95 | 0.20 (1.4%) | 0.43 (3.1%) | 0.12 (0.8%) | 11.98 (85.9%) | 1.22 (8.7%) |

**Table 4.** Natural Event Tracer Percent Recoveries and the Total Percentage of Water Recovered for the 12-m and 30-m Application of NaCl

| | Section 1 (%) | Preferential 1 (%) | Section 2 (%) | Pipe 2A (%) | Pipe 2B (%) | Section 3 (%) | Total Recovery (%) |
|---|---|---|---|---|---|---|---|
| | | | *12-m Tracer Test* | | | | |
| Tracer | 0.5 | 0.3 | 0.1 | 94.7 | 4.4 | 0.0 | 19.8 |
| Water | 8.3 | 13.6 | 3.5 | 63.5 | 7.3 | 3.8 | |
| | | | *30-m Tracer Test* | | | | |
| Tracer | 9.1 | 3.9 | 0.6 | 77.7 | 7.3 | 1.4 | 24.2 |
| Water | 13.6 | 12.2 | 3.0 | 61.8 | 5.6 | 3.9 | |

under different steady state flow rates and during different rainfall conditions. The results showed that the rainfall intensity and the pumping rate affected the subsurface flow velocity. When experiments are conducted to determine the subsurface flow velocity of a hillslope with preferential flow features it is important to consider the boundary conditions, slope length, flow rate, and precipitation conditions because these factors will affect the measured tracer velocities [*Brooks et al.*, 2004].

### 4.3. Conceptual Models of Hillslope Preferential Flow

[42] To put experimental results in context and validate models we need to understand the relation between hillslope subsurface flow velocities, soil moisture and input parameters such as rainfall conditions, antecedent conditions and piezometer pore water pressures. The general concept of lateral preferential flow networks is that increasing soil moisture or locally higher water table levels increase the number of preferential connections in a generally disconnected network, which causes faster subsurface velocities and an increase in the area of hillslope contributing to subsurface flow [*Sidle et al.*, 2000; *Tromp-van Meerveld and McDonnell*, 2006b; *Tsuboyama et al.*, 1994; *Uchida et al.*, 2005]. This often results in threshold behavior that should be apparent in the relation between the velocity and the most dominant factors affecting the soil moisture and the connectivity between preferential features. The best relation among the different factors influencing flow velocities in this study is between the velocity and the 1-h rainfall intensity (Figure 7). While this appears to be contrary to other results and conceptual models that show that subsurface flow volume is related to antecedent condition [*Sidle et al.*, 2000] or total rainfall volume [*Tromp-van Meerveld and McDonnell*, 2006b], our study focuses instead on subsurface flow velocity and its relation to controlling factors. There appears to be a precipitation intensity threshold of approximately 5 mm/h below which the hillslope velocity changes by an order of magnitude and above which the velocity is relatively constant. This strong relation at the Russell Creek site could be an artifact of the surface application of the tracer, or it could be that the dominant process is the storm intensity threshold that is required to initiate fast vertical percolation of water. The rapid percolation would then increase the soil moisture at depth, causing fast hillslope flows (Figure 7).

[43] The connections between preferential flow features are assumed to increase with soil moisture. Moisture in the soil is governed by the rainfall (and snowmelt) characteristics and the antecedent moisture condition. These experiments were conducted during wet winter and spring conditions, when soils are likely to be at or near field capacity most of the time. Under these conditions we expected antecedent moisture condition to have little influence on the connections between preferential flow features. Although we did not measure soil moisture directly we calculated several indices of antecedent moisture condition and found that the 7-day antecedent precipitation index (API) was best correlated with the velocities. Similar to the findings of other studies [e.g., *Kienzler and Naef*, 2008], as a standalone parameter API was not an important factor controlling the subsurface flow velocity. However, when taken as one factor in a multiple regression, it became marginally significant at a type-1 error probability of 10%. It is therefore likely that if these measurements were conducted over the course of a year, antecedent moisture condition would become a more important control over subsurface velocities because a broader range of antecedent moisture conditions would occur owing to fewer storms and higher evapotranspiration in summer and fall.

[44] Hillslopes that are dominated by preferential networks usually experience overland flow only in areas of flow convergence, such as topographical hollows, because of the high capacity of the preferential flow network to drain the soil

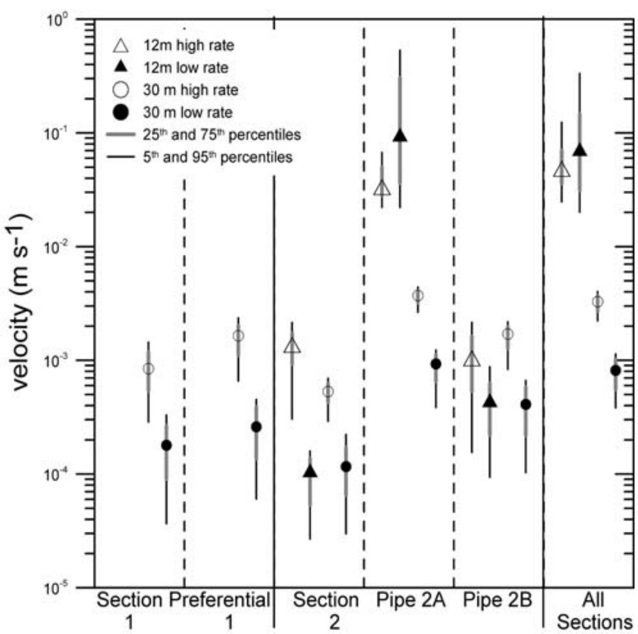


**Figure 5.** Forced experimental results for each gauged section and the entire hillslope. Average velocities are derived from the advection-dispersion equation, and the tenth and ninetieth uncertainty percentiles are derived from the GLUE methodology.

**Table 5.** Measured Hillslope Velocities With Selected Storm Parameters and Velocities Predicted by Regression Equations

| Event | Date | Total P (mm) | Total Q ($m^3$) | 7-Day API (mm) | 1-h Rainfall Intensity R1 (mm/h) | Hillslope Velocity V (m/s) | D | V-calc1 | V-calc2 |
|---|---|---|---|---|---|---|---|---|---|
| 1 | 7 Mar | 14 | 16.3 | 35 | 5 | 0.001200 | 1 | 0.000437 | 0.001173 |
| 2 | 10 Mar | 10 | 0.5 | 65 | 2.5 | 0.000046 | 0 | 0.000000 | 0.000000 |
| 3 | 16 Mar | 27 | 5.8 | 55 | 4 | 0.000025 | 0 | 0.000309 | 0.000150 |
| 4 | 25 Mar | 41 | 29.1 | 39 | 3.8 | 0.000248 | 0 | 0.000201 | 0.000076 |
| 5 | 30 Mar | 87 | 98 | 60 | 8.2 | 0.000546 | 0 | 0.001216 | 0.000686 |
| 6 | 5 Apr | 104 | 97.6 | 108 | 4.8 | 0.001390 | 1 | 0.000698 | 0.001369 |
| 7 | 10 Apr | 19 | 1.8 | 154 | 2.4 | 0.000287 | 0 | 0.000383 | 0.000251 |
| 8 | 15 Apr | 45 | 49.6 | 98 | 7.3 | 0.001720 | 1 | 0.001184 | 0.001649 |
| 9 | 10 May | 27 | 2 | 4 | 12.1 | 0.002070 | 1 | 0.001807 | 0.001960 |
| 10 | 14 May | 15 | 0.8 | 36 | 4.1 | 0.000069 | 0 | 0.000252 | 0.000104 |
| 11 | 18 May | 58 | 33 | 49 | 4.8 | 0.000208 | 0 | 0.000453 | 0.000231 |
| 12 | 21 May | 92 | 81.3 | 104 | 7.6 | 0.000713 | 0 | 0.001272 | 0.000745 |
| 13 | 17 Jun | 16 | 10.8 | 36 | 4 | 0.000202 | 0 | 0.000230 | 0.000092 |

[*Fannin et al.*, 2000]. The ability of water to exploit different preferential features was shown by results of the 30-m forced experiment, where an increase in the flow rate caused different subsurface features to compensate for the additional water and redirect water away from S2 to S1. It was not the maximum capacity of the features in S2 (pipe 2A in particular) that limited the flow during 30 mHR because (1) the measurements of flow from pipe 2A under natural events exceeded 30 L/min (Figure 4), (2) the 12-m high-rate experiment transmitted 28 L/min through pipe 2A (Table 3), and (3) both flow rates are more than the 30 mHR steady state input rate of 23.5 L/min (Table 3). The redirection of water from S2 to S1 could be caused by the preferential flow network that transmits water to S2 reaching its maximum capacity, after which additional water exploited features that routed water to S1. This might also explain the rapid change in flow rate seen in S1 during large natural events. It is possible that S1 does not connect to another part of the hillslope, but that features in the upper 18 m of the hillslope diverted water and tracer into S1 once their maximum capacity to deliver water to S2 had been reached, such as described by *Sidle et al.* [2000].

[45] Application methods such as ponded water or water injected from a line source could affect the pore water pressure around the injection sites and increase flow through preferential flow features, or access flow features high in the soil profile that may not be active under natural conditions. We measured the depth of water in the trenches with a pressure transducer; for the 12-m experiment, the trench had an 80-mm difference in water depth between the high and the low rate, while for the 30-m experiment there was no difference in elevation head between the two pumping rates. We assumed that there was no change in the elevation head in the 30-m trench because, similar to the peizometers that drained too quickly for slug injection, the water could flow into an area of high hydraulic conductivity which was more than our application rate of water (e.g., a preferential flow feature). The increase in water depth could have increased the pressure head driving the flow for the 12-m application; however, the measured velocities were unchanged. This suggests either (1) that the 12-m section was composed of highly connected, large features that had little exchange with the surrounding hillslope, or (2) that in the 12-m section of hillslope the number of active preferential features had increased. Conservation of mass (Q = VA) suggests that the area of flow changed as the velocity was constant. Excavations and dye staining at the Russell Creek site later revealed that this section of hillslope was composed of large features (up to 30 cm in width, and up to 3 m long) and connected by fine gravel material [*Anderson et al.*, 2009]. The surrounding soil was much finer textured with higher clay content and showed little staining. Reducing the pumping rate (12 mHR compared to 12 mLR, Figure 5) had no significant effect on the velocity of the tracer through pipe 2A or the depth of water in the trench, but the velocity through S2 was reduced. At the high-flow rate the preferential features could have been close to their maximum capacity, which would create a large pressure gradient in the surrounding soil matrix and cause faster flows through the soils surrounding pipe 2A (Figure 5 and Table 2).

[46] These results suggest that there are potentially two conceptual types of preferential flow networks, corresponding to the two distinct topographic units that made

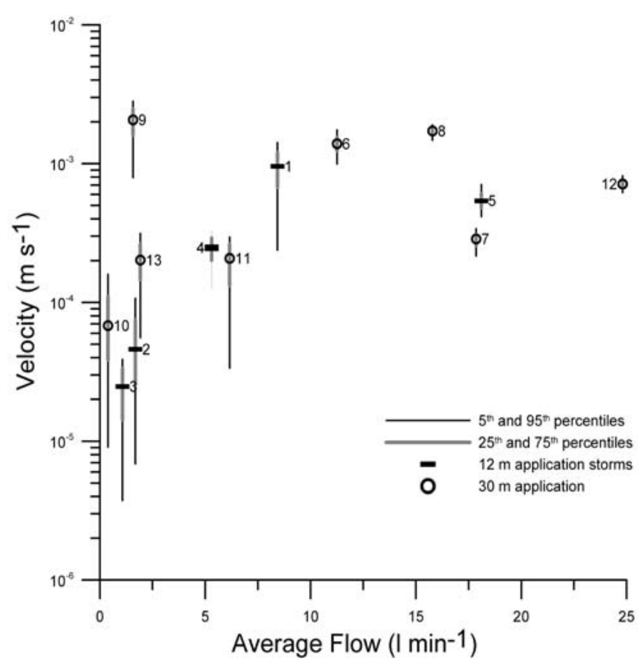


**Figure 6.** Average velocity for the 13 storms and the 4 forced experiments versus the average flow rate for each storm. Error bounds are uncertainty as defined in Figure 5.

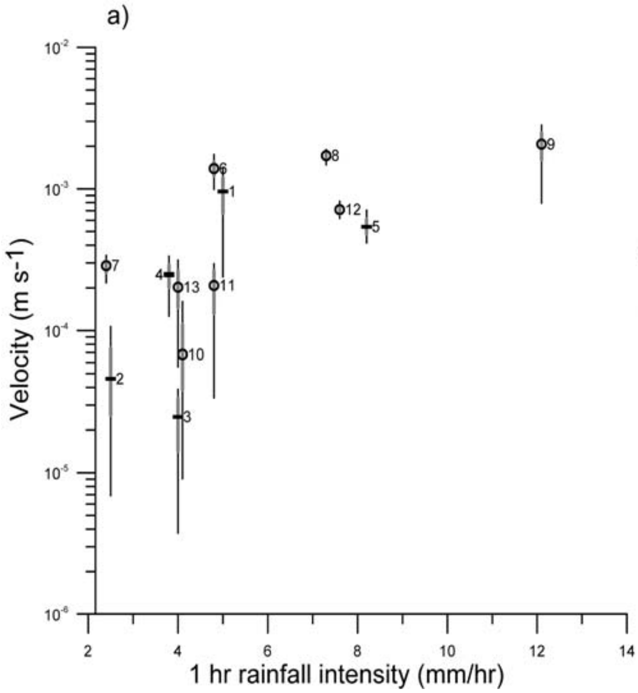


**Figure 7.** Average velocity for the 13 storms versus (a) the 1-h maximum rainfall intensity and (b) the total storm rainfall. Note that storm 3 contains snowmelt. Error bounds are uncertainty as defined in Figure 5.

up the experimental hillslope at Axel Creek: the topographic hollows, characterized by convergent flows and fine-grained soils, and the convex hillslope sections with divergent flows and coarser-grained soils. In the topographical hollow above S2 we observed large preferential features that were connected by isolated lenses of coarse soil (fine gravels), while the convex hillslope sections above S1 and S3 were characterized by small preferential flow features connected by mineral and fibrous organic soils [*Anderson et al.*, 2009] which are similar to the systems described by *Sidle et al.* [2000]. S2 and the preferential features behaved as conceptual pipes, having little interaction with the surrounding soil matrix. Generally, the preferential flow paths in the topographic hollow carry most of the preferential flow from the

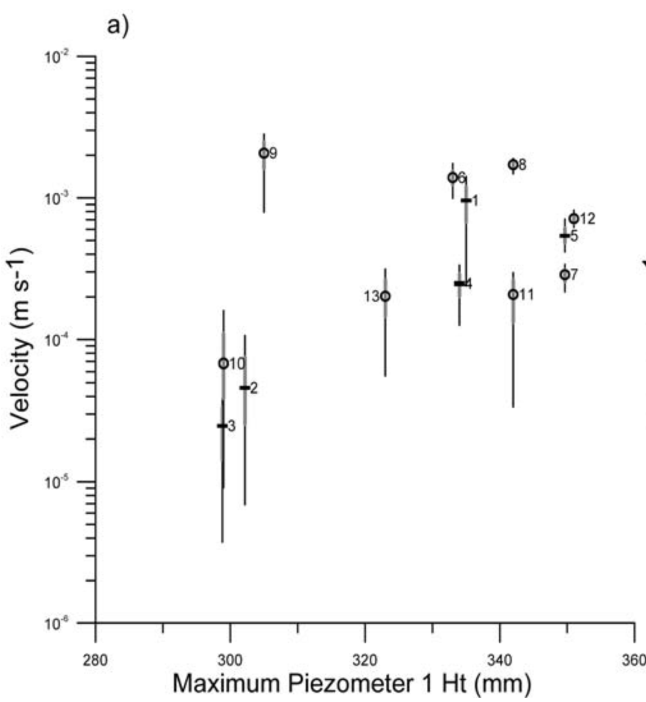


**Figure 8.** Average velocity for the 13 storms versus the maximum water table height for (a) piezometer 1 and (b) piezometer 2. Error bounds are uncertainty as defined in Figure 5.

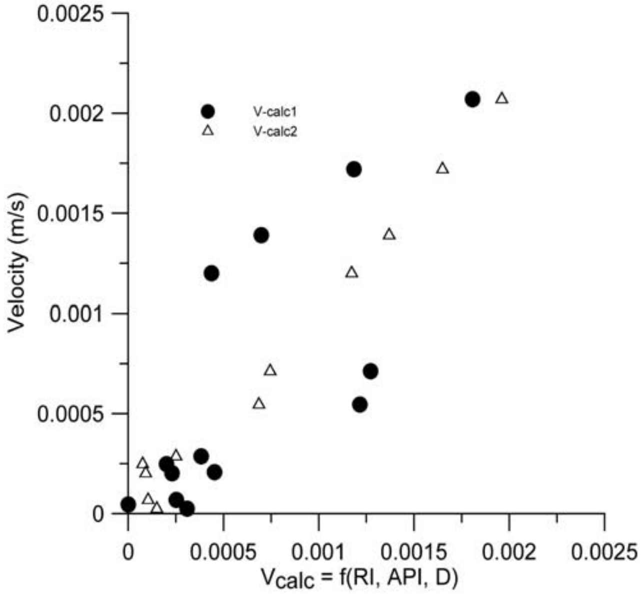


**Figure 9.** Measured velocity versus velocity calculated from regression equations, where V-calc1 and V-calc2 are the regressions without and with the classification variable.

entire hillslope, and the soils in the topographic hollow carry most of the matrix flow. However, once a threshold flow was reached (about 30 L/min for Pipe 2A in Figure 4) it is possible that connections to features in S1 caused a dramatic increase in the flow rate through features in the convex sections (S1 and preferential flow 1 in Figure 4).

[47] The strong relationship between the response of piezometer P2 and the velocity (Figure 8) is believed to be due to the proximity of the piezometer to one of the large features in this preferential flow network. Excavation of the hillslope revealed that piezometer P2 was close to a major preferential flow feature. It responded during the forced experiments, while other piezometers did not respond. A slug test could not be performed on piezometer P2 because the water drained too quickly to conduct the test, suggesting that it was completed in a gravel lens. The dynamic response of P2 to storm inputs is indicative of the wide range of soil water conditions created by the large preferential flow paths.

**Table 6.** Results of Multiple Regression Analysis of Subsurface Flow Velocity V Against 1-h Rainfall Intensity R1 and 7-Day API[a]

| | Coefficient | SD | *t* Ratio | p |
|---|---|---|---|---|
| $V_{calc1} = -0.000763 + 0.000211\ R1 + 0.000004\ API$ | | | | |
| Constant | −0.00069320 | 0.00039520 | −1.75 | 0.110 |
| R1 | 0.00018379 | 0.00004761 | 3.86 | 0.003 |
| API | 0.00000476 | 0.00000317 | 1.50 | 0.165 |
| Standard error | | 0.0004559 | F score | 8.51 |
| Adjusted $R^2$ (%) | | 55.6 | p | 0.007 |
| $V_{calc2} = -0.000513 + 0.000124\ R1 + 0.000003\ API + 0.000960\ D$ | | | | |
| Constant | −0.00051310 | 0.00011780 | −4.35 | 0.002 |
| R1 | 0.00012435 | 0.00001595 | 7.80 | 0.000 |
| API | 0.00000303 | 0.00000093 | 3.25 | 0.010 |
| D | 0.00095956 | 0.00008536 | 11.24 | 0.000 |
| Standard error | | 0.0001239 | F score | 118.90 |
| Adjusted $R^2$ (%) | | 96.7 | p | 0.000 |

[a]API, antecedent precipitation index.

**Table 7.** Average Velocities Measured During Selected Experiments

| | Velocity Range (m/h) | | |
|---|---|---|---|
| Distance (m) | Minimum | Maximum | Reference |
| 4 | 4.3 | 154.8 | *Mosley* [1979] |
| 1 | 10.8 | | *Mosley* [1982] |
| 2 | 0.4 | 0.6 | *Tsuboyama et al.* [1994] |
| 10/13.5 | 7.8 | 24.0 | *Mikovari et al.* [1995] |
| 35–40 | 0.4 | 0.5 | *Nyberg et al.* [1999] |
| 35–40 | 2.4 | 2.5 | *Nyberg et al.* [1999] |
| 3 | 4.3 | 22.7 | *Hetherington* [1995] |
| 3 | 33.1 | 165.6 | *Hetherington* [1995] |
| 7.7 | 2.5 | 32.4 | *Weiler et al.* [1998] |
| 8.3 | 0.8 | 2.9 | *Weiler et al.* [1998] |
| | 10.8 | 13.3 | *Feyen et al.* [1999][a] |
| | 0.6 | 3.4 | *Feyen et al.* [1999][a] |
| 2 | 8.6 | 13.7 | *Noguchi et al.* [1999] |
| 4/8 | 7.2 | 10.8 | *Retter* [2007] |
| 30/12 | 2.9 | 331.2 | this study, forced |
| 30/12 | 0.1 | 7.6 | this study, natural conditions |

[a]Unable to determine the distances.

[48] Unlike a matrix flow system operating under Darcy's Law where the cross-sectional saturated area of flow determines the velocity and flow rate, in a hillslope with a preferential flow network the flow characteristics are affect by the number and type of preferential features connected within the network. Features and material that create the preferential network are important in determining how the water table, hillslope discharge, and subsurface velocity will behave and how best to model a particular hillslope. Like the hydraulic conductivity of soils, the preferential features and connecting material vary between hillslopes, depending on the processes that create and modify them. Factors influencing the preferential network include climate, soil, topography, contributing area, and physical/mechanical processes (burrowing animals, insects, worms, roots, subsurface erosion, etc.) [*Tsuboyama et al.*, 1994].

[49] The hillslope processes in this study watershed and others with similar climate and topography are dominated by large highly connected preferential flow features that are created and maintained by large amounts of water moving through shallow soils (0.5–2 m). These preferential flow networks are even activated during small storms at times when soils are maintained at or near field capacity by high precipitation and low evaporation. Models that reflect this dynamic hillslope behavior are better suited for hillslopes with these efficient preferential flow networks [e.g., *Weiler and McDonnell*, 2007]. Other hillslopes may have less developed preferential flow networks that are only activated during high antecedent conditions or under certain precipitation conditions [*Uchida et al.*, 2005]. To properly model and manage watersheds, it is important to be able to classify the type of hillslope response [*Uchida et al.*, 2005]. Steep hillslopes with shallow soils, high-rainfall regimes and no evidence of surface runoff are likely to have well developed preferential features and efficient preferential flow networks similar to that of the Russell Creek experimental hillslope.

## 5. Summary and Conclusions

[50] A hillslope with known preferential flow paths was instrumented and set up to measure subsurface flows by a

variety of methods. Piezometers were installed within the hillslope and all outflows from the hillslope, including matrix flow and flow from preferential flow paths, were collected and measured at a road cut. Nearby meteorological instrumentation and streamflow gauges provided additional information. NaCl tracer was applied to the slope under natural and steady state boundary conditions to determine subsurface lateral flow velocities. The results of the tracer experiments were used to determine the relationship between the tracer velocities and the independent parameters of slope length, steady state inflow rate, piezometer response, and storm characteristics.

[51] The measured subsurface flow velocities at the Russell Creek hillslope were among the highest reported in the literature from forest and grassland sites around the world. They were closely related to the 1-h rainfall intensity, but only marginally related to antecedent moisture conditions owing to the limited range of those conditions during the experiments. In addition, our site had a very small water table response. These findings suggest that the preferential flow network at this site operates completely independently from the soil matrix and carries most of the subsurface flow during storms. Further, the velocities were higher when measured over a short distance (i.e., 12 m) than a larger distance (i.e., 30 m). Because of the ephemeral nature of the connections between preferential flow features, the flow paths were more likely to be connected over the shorter than the longer distance. This explains the difference in flow velocity with distance and suggests that the connectivity of the hillslope preferential flow network is an important factor governing the average subsurface flow velocity.

[52] **Acknowledgments.** The British Columbia Forest Investment Account and the Natural Sciences and Engineering Research Council of Canada provided funding for this project.

## References

Anderson, A. E., et al. (2009), Dye staining and excavation of a lateral preferential flow network, *Hydrol. Earth Syst. Sci.*, *5*, 1043–1065.

Beckers, J., and Y. Alila (2004), A model of rapid preferential hillslope runoff contributions to peak flow generation in a temperate rain forest watershed, *Water Resour. Res.*, *40*, W03501, doi:10.1029/2003WR002582.

Beven, K., and J. Freer (2001), Equifinality, data assimilation, and uncertainty estimation in mechanistic modelling of complex environmental systems using the GLUE methodology, *J. Hydrol.*, *249*(1–4), 11–29, doi:10.1016/S0022-1694(01)00421-8.

Brooks, E. S., et al. (2004), A hillslope-scale experiment to measure lateral saturated hydraulic conductivity, *Water Resour. Res.*, *40*, W04208, doi:10.1029/2003WR002858.

Faeh, A. O., et al. (1997), A combined field and numerical approach to investigate flow processes in natural macroporous soils under extreme precipitation, *Hydrol. Earth Syst. Sci.*, *1*, 787–800.

Fannin, R. J., et al. (2000), Hydrologic response of soils to precipitation at Carnation Creek, British Columbia, Canada, *Water Resour. Res.*, *36*(6), 1481–1494, doi:10.1029/2000WR900027.

Feyen, H., et al. (1999), A tracer experiment to study flow paths of water in a forest soil, *J. Hydrol.*, *225*(3–4), 155–167, doi:10.1016/S0022-1694(99)00159-6.

Hetherington, E. D. (1995), Subsurface water flow rates over bedrock on steep slopes in the Carnation Creek experimental watershed, in *Mountain Hydrology: Peaks and Valleys in Research and Application, and Forest Meteorology*, edited by B. T. Guy and J. Barnard, pp. 17–21, Can. Water Resour. Assoc., Cambridge, Ont., Canada.

Hudson, R., and J. Fraser (2005), Introduction to salt dilution gauging for streamflow measurement, Part IV: The mass balance (or dry injection) method, *Streamline Watershed Manage. Bull.*, *9*(1), 6–12.

Hutchinson, D. G., and R. D. Moore (2000), Throughflow variability on a forested hillslope underlain by compacted glacial till, *Hydrol. Processes*, *14*(10), 1751–1766, doi:10.1002/1099-1085(200007)14:10<1751::AID-HYP68>3.0.CO;2-U.

Kienzler, P. M., and F. Naef (2008), Subsurface storm flow formation at different hillslopes and implications for the 'old water paradox', *Hydrol. Processes*, *22*(1), 104–116, doi:10.1002/hyp.6687.

Kim, H. J., et al. (2004), Throughflow variability during snowmelt in a forested mountain catchment, coastal British Columbia, Canada, *Hydrol. Processes*, *18*(7), 1219–1236, doi:10.1002/hyp.1396.

Kitahara, H. (1993), Characteristics of pipe flow in forested slopes, *IAHS Publ.*, *212*, 235–242.

Kung, K. J. S., et al. (2005), Quantifying pore-size spectrum of macropore-type preferential pathways, *Soil Sci. Soc. Am. J.*, *69*(4), 1196–1208, doi:10.2136/sssaj2004.0208.

Kung, K. J. S., et al. (2006), Quantifying the pore size spectrum of macropore-type preferential pathways under transient flow, *Vadose Zone J.*, *5*(3), 978–989, doi:10.2136/vzj2006.0003.

Maloszewski, P. (1994), Mathematical modelling of tracer experiments in fissured aquifers, *Freiburger Schr. Hydrol.*, *2*, 107 pp.

Mikovari, A., et al. (1995), Investigation of preferential flow using tracer techniques, *IAHS Publ.*, *229*, 183–192.

Minitab Inc. (1995), *Minitab Reference Manual*, State College, Pa.

Mosley, M. P. (1979), Streamflow generation in a forested watershed, New Zealand, *Water Resour. Res.*, *15*(4), 795–806, doi:10.1029/WR015i004p00795.

Mosley, M. P. (1982), Subsurface flow velocities through selected forest soils, South Island, New Zealand, *J. Hydrol.*, *55*(1–4), 65–92, doi:10.1016/0022-1694(82)90121-4.

Nash, J., and J. Sutcliffe (1970), River flow forecasting through conceptual models–Part 1: A discussion of principles, *J. Hydrol.*, *10*(3), 282–290, doi:10.1016/0022-1694(70)90255-6.

Noguchi, S., et al. (1999), Morphological characteristics of macropores and the distribution of preferential flow pathways in a forested slope segment, *Soil Sci. Soc. Am. J.*, *63*(5), 1413–1423.

Nyberg, L., et al. (1999), Water transit times and flow paths from two line injections of H-3 and $Cl^{-}36$ in a microcatchment at Gardsjon, Sweden, *Hydrol. Processes*, *13*(11), 1557–1575, doi:10.1002/(SICI)1099-1085(19990815)13:11<1557::AID-HYP835>3.0.CO;2-S.

Parlange, M. B., et al. (1989), Subsurface flow above a fragipan horizon, *Soil Sci.*, *148*(2), 77–86, doi:10.1097/00010694-198908000-00001.

Peters, D. L., et al. (1995), Runoff production in a forested, shallow soil, Canadian Shield Basin, *Water Resour. Res.*, *31*(5), 1291–1304, doi:10.1029/94WR03286.

Retter, M. (2007), *Surface Flow Formation*, Univ. Bern, Bern.

Roberge, J., and A. P. Plamondon (1987), Snowmelt runoff pathways in a boreal forest hillslope: The role of pipe throughflow, *J. Hydrol.*, *95*(1–2), 39–54, doi:10.1016/0022-1694(87)90114-4.

Ronkanen, A. K., and B. Klove (2007), Use of stabile isotopes and tracers to detect preferential flow patterns in a peatland treating municipal wastewater, *J. Hydrol.*, *347*(3–4), 418–429, doi:10.1016/j.jhydrol.2007.09.029.

Roth, K., and W. A. Jury (1993), Modeling the transport of solutes to groundwater using transfer-functions, *J. Environ. Qual.*, *22*(3), 487–493.

Sidle, R. C. (2006), Field observations and process understanding in hydrology: Essential components in scaling, *Hydrol. Processes*, *20*(6), 1439–1445, doi:10.1002/hyp.6191.

Sidle, R. C., et al. (1995), Seasonal hydrologic response at various spatial scales in a small forested catchment, Hitachi-Ohta, Japan, *J. Hydrol.*, *168*(1–4), 227–250, doi:10.1016/0022-1694(94)02639-S.

Sidle, R. C., et al. (2000), Stormflow generation in steep forested headwaters: A linked hydrogeomorphic paradigm, *Hydrol. Processes*, *14*(3), 369–385, doi:10.1002/(SICI)1099-1085(20000228)14:3<369::AID-HYP943>3.0.CO;2-P.

Sidle, R. C., et al. (2001), A conceptual model of preferential flow systems in forested hillslopes: Evidence of self-organization, *Hydrol. Processes*, *15*(10), 1675–1692, doi:10.1002/hyp.233.

Steenhuis, T. S., et al. (1988), Preferential flow influences on drainage of shallow sloping soils, *Agric. Water Manage.*, *14*(1–4), 137–151, doi:10.1016/0378-3774(88)90069-8.

Tani, M. (1997), Runoff generation processes estimated from hydrological observations on a steep forested hillslope with a thin soil layer, *J. Hydrol.*, *200*(1–4), 84–109, doi:10.1016/S0022-1694(97)00018-8.

Terajima, T., et al. (2000), Morphology, structure and flow phases in soil pipes developing in forested hillslopes underlain by a Quaternary sand-gravel formation, Hokkaido, northern main island in Japan, *Hydrol. Processes*, *14*(4), 713–726, doi:10.1002/(SICI)1099-1085(200003)14:4<713::AID-HYP968>3.0.CO;2-T.

Tromp-van Meerveld, H. J., and J. J. McDonnell (2006a), Threshold relations in subsurface stormflow: 1. A 147-storm analysis of the Panola hillslope, *Water Resour. Res.*, *42*, W02410, doi:10.1029/2004WR003778.
Tromp-van Meerveld, H. J., and J. J. McDonnell (2006b), Threshold relations in subsurface stormflow: 2. The fill and spill hypothesis, *Water Resour. Res.*, *42*, W02411, doi:10.1029/2004WR003800.
Tsuboyama, Y., et al. (1994), Flow and solute transport through the soil matrix and macropores of a hillslope segment, *Water Resour. Res.*, *30*(4), 879–890, doi:10.1029/93WR03245.
Tsukamoto, Y., and T. Ohta (1988), Runoff process on a steep forested slope, *J. Hydrol.*, *102*(1–4), 165–178, doi:10.1016/0022-1694(88)90096-0.
Tsutsumi, D., et al. (2005), Development of a simple lateral preferential flow model with steady state application in hillslope soils, *Water Resour. Res.*, *41*, W12420, doi:10.1029/2004WR003877.
Uchida, T., et al. (1999), Runoff characteristics of pipeflow and effects of pipeflow on rainfall-runoff phenomena in a mountainous watershed, *J. Hydrol.*, *222*(1–4), 18–36, doi:10.1016/S0022-1694(99)00090-6.
Uchida, T., et al. (2005), The role of lateral pipe flow in hillslope runoff response: An intercomparison of non-linear hillslope response, *J. Hydrol.*, *311*(1–4), 117–133, doi:10.1016/j.jhydrol.2005.01.012.
Weiler, M., and J. McDonnell (2004), Virtual experiments: A new approach for improving process conceptualization in hillslope hydrology, *J. Hydrol.*, *285*(1–4), 3–18, doi:10.1016/S0022-1694(03)00271-3.
Weiler, M., and J. J. McDonnell (2007), Conceptualizing lateral preferential flow and flow networks and simulating the effects on gauged and ungauged hillslopes, *Water Resour. Res.*, *43*, W03403, doi:10.1029/2006WR004867.
Weiler, M., et al. (1998), Study of runoff generation on hillslopes using tracer experiments and a physically based numerical model, *IAHS Publ.*, *248*, 353–360.
Weiler, M., et al. (2005), Subsurface stormflow, *Encycl. Hydrol. Sci.*, *3*, 1719–1732.
Zhang, D. R., et al. (2006), A comparison of non-linear least square and GLUE for model calibration and uncertainty estimation for pesticide transport in soils, *Adv. Water Resour.*, *29*(12), 1924–1933, doi:10.1016/j.advwatres.2006.02.004.

Y. Alila and R. O. Hudson, Department of Forest Resources Management, University of British Columbia, Vancouver, BC V6T 1Z4, Canada.
A. E. Anderson, Sustainable Resource Development, 8660 Bearspaw Dam Road NW, Calgary, AB T3L 1S4, Canada. (axel.anderson@gov.ab.ca)
M. Weiler, Institute of Hydrology, Albert-Ludwigs University of Freiburg, D-79085 Freiburg, Germany.